ORGANIC CHEMISTRY FRONTIERS

CCS 中国化学会 CHINESE CHEMICAL SOCIETY

SIOC 1950

ROYAL SOCIETY OF CHEMISTRY

RESEARCH ARTICLE

View Article Online
View Journal | View Issue

Cite this: *Org. Chem. Front.*, 2022, **9**, 929

Planar Blatter radicals through Bu_3SnH- and TMS_3SiH-assisted cyclization of aryl iodides: azaphilic radical addition†

Paulina Bartos, *[a] Małgorzata Celeda, [a] Anna Pietrzak [b] and Piotr Kaszyński *[a,c,d]

Received 22nd November 2021,
Accepted 9th December 2021

DOI: 10.1039/d1qo01742j

rsc.li/frontiers-organic

Bu_3SnH- and TMS_3SiH-assisted cyclizations of iodoarene derivatives of benzo[*e*][1,2,4]triazine lead to the formation of planar Blatter radicals (2-phenyl-3*H*-[1,2,4]triazino[5,6,1-*kl*]phenoxazin-3-yls and 2-phenyl-3*H*-[1,2,4]triazino[5,6,1-*kl*]phenothiazin-3-yls) in yields of up to 96%. The cyclization step involves the thermodynamically favored (DFT: $\Delta G^{\ddagger}_{298}$ = 3.1 kcal mol^{-1} and ΔH = −55.3 kcal mol^{-1}) unprecedented attack of a C-centered radical on the heterocyclic N atom. This method opens up access to functionalized sulfur-containing planar Blatter radicals for the first time. New radicals were characterized using spectroscopic (UV–vis, EPR), electrochemical, and single-crystal X-ray diffraction methods.

Introduction

Increasing interest in stable radicals as structural elements for advanced materials[1–8] has resulted in increasing demand for their functional derivatives with tailored properties. Of particular interest is the benzo[*e*][1,2,4]triazinyl radical (Blatter radical)[9] and its derivatives,[10,11] which are exceptionally stable,[12,13] and exhibit π-spin delocalization,[14] a narrow electrochemical window,[15,16] and low excitation energies.[17] For these reasons, there is rapidly increasing interest in the exploration of this radical as a structural element for advanced materials, such as sensors,[18] photodetectors[19] and liquid crystalline photoconductors,[20,21] and also for applications in spintronics[22–24] and radical polymerization.[25,26]

Recent advances[10,11] in the chemistry of the benzo[*e*][1,2,4]triazinyl led to the discovery of planar Blatter radicals.[27] The two parent radicals, **1O-a** (2-Ph-3*H*-[1,2,4]triazino[5,6,1-*kl*]phenoxazin-3-yl) containing a phenoxazine ring and **1S-a** based on phenothiazine (2-phenyl-3*H*-[1,2,4]triazino[5,6,1-*kl*]phenothiazin-3-yl), were obtained in low yields (20–25%) *via* the intramolecular azaphilic addition of ArLi, which was generated *in situ* from the appropriate derivative **2-a** (Method A, Fig. 1).[27] A much improved yield of **1O-a** and access to its functional derivatives were demonstrated with the aza-Pschorr cyclization reaction (Method B).[28–31] Further progress in the synthesis of ring-fused derivatives of **1O-a** involved photocyclization (Mallory-type cyclization) of C(8)-substituted benzo[*e*][1,2,4]triazines (Method C, Fig. 1).[32] Unfortunately, neither of the latter two methods is suitable for the preparation of sulfur-containing radicals **1S:** strongly oxidative conditions are incompatible with the divalent sulfur in Method B, while in Method C the heavy atom effect causes a rapid decay of the S_1 state.

Successful Pschorr cyclization (Method B) implies an azaphilic addition of the transient aryl radical to the [1,2,4]triazine and suggests that other processes involving aryl rad-

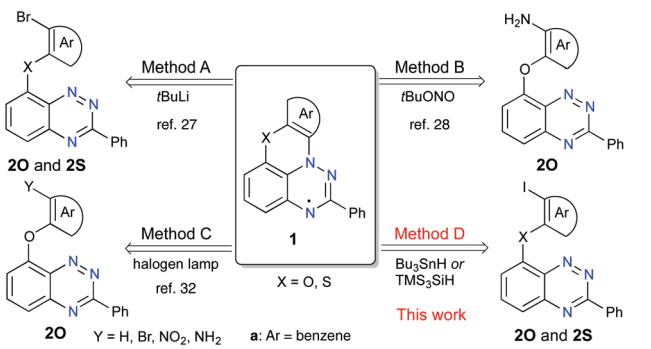

Fig. 1 Three known (A–C) methods and one new (D) method for the preparation of planar benzo[*e*][1,2,4]triazin-4-yl radicals **1O** and **1S**.

[a]*Faculty of Chemistry, University of Łódź, 91-403 Łódź, Poland. E-mail: piotr.kaszynski@chemia.uni.lodz.pl*
[b]*Faculty of Chemistry, Łódź University of Technology, 90-924 Łódź, Poland*
[c]*Centre of Molecular and Macromolecular Studies, Polish Academy of Sciences, 90-363 Łódź, Poland*
[d]*Department of Chemistry, Middle Tennessee State University, Murfreesboro, Tennessee 37132, USA*

†Electronic supplementary information (ESI) available: Additional synthetic details, NMR spectra, details of XRD, spectroscopic (UV-vis and EPR) and electrochemical analyses and archives of DFT computational results. CCDC 2107124. For ESI and crystallographic data in CIF or other electronic format see DOI: 10.1039/d1qo01742j

icals,[33] *e.g.* transformations of aryl halides in the presence of R_3SnH[34,35] or R_3SiH,[36,37] could also lead to *N*-cyclization and formation of the planar radical.

Radical chain cyclization reactions[38,39] of aryl halides in the presence of R_3SnH[34,35] or R_3SiH[36,37] are well-established and have been used for the formation of carbocyclic derivatives (*e.g.* phenanthrenes[40–42] and helicenes[43,44]) and for a variety of ring-fused heterocycles.[38,39,45–48] In all these reactions, the key step is the attack of the transient C-centered radical onto the ring C-atom, which is preferred over the N-attack, if the two paths are available.[49,50] Consequently, N-attack of an aryl radical has never been observed in tin- or silicon-hydride-assisted radical cyclization processes.

Herein, we present an efficient Bu_3SnH- and TMS_3SiH-assisted radical chain cyclization of aryl iodides **2** on the [1,2,4]triazine N-atom and the formation of planar Blatter radicals **1O** and **1S** (Method D, Fig. 1). The new method is tested on four previously reported radicals and applied to the preparation of the first functionalized sulfur-containing planar Blatter radical, ester **1S-b**, as well as **1O-c**. The two newly obtained radicals, **1O-c** and **1S-b**, are characterized by spectroscopic (UV-vis and EPR) and electrochemical methods, and the structure of the former radical is determined using a single crystal XRD method.

Results and discussion

Synthesis

Initial investigation focused on the cyclization reaction of the benzo[*e*][1,2,4]triazine **2O-a** with Bu_3SnH in toluene (Fig. 2). Following a literature procedure for similar cyclization reactions,[39,44] a solution of the initiator AIBN was added to a solution of **2O-a** and Bu_3SnH in toluene at 80 °C over a 4 h period *via* a syringe pump (Method D-Sn). The initially formed *leuco* form, **1O-a-*leuco***, underwent slow oxidation to **1O-a** during workup, and more rapidly during deposition onto the passivated SiO_2. The crude radical **1O-a**, which was isolated by filtration through passivated silica gel, contained significant amounts of organotin impurities. Therefore, following a modified analogous procedure[24] crude **1O-a** was oxidized with AgOTf to $[\mathbf{1O\text{-}a}]^+$, which was purified using chromatography. The pure salt was subsequently reduced with Zn/AcOH and the resulting **1O-a-*leuco*** was exposed to air, giving pure radical **1O-a** in 48–52% yield (Scheme 1). Using the same method, radicals **1O-b**, **1O-c** and **1S-a** were obtained in comparable yields of 42–69% (Fig. 2). The yield of radical **1O-d** was significantly lower than those of the others in the series (13% yield), mainly due to its lower stability on silica gel and alumina during the purification process.

The difficulties with the removal of organotin byproducts prompted the investigation of an alternative method using TMS_3SiH instead of Bu_3SnH. Thus, treatment of benzo[*e*][1,2,4]triazine **2O-a** with TMS_3SiH in toluene in the presence of AIBN gave the desired radical **1O-a** in an excellent yield of 96% (Method D-Si) without the need of going through the cation $[\mathbf{1O\text{-}a}]^+$ for purification purposes. This method allowed radicals **1O-a**–**1O-c** and the parent sulfur-containing radical **1S-a** to be obtained in higher yields of 48–94%. This method appears to be superior to Method D-Sn, and therefore was used to obtain radical **1S-b**, the first functional derivative of **1S-a**. The same Method D-Si did not work unfortunately for the extended radical **1O-d**. The starting **2O-d** was fully consumed, and only a complex mixture of polar products was formed.

The parent radicals **1O-a** and **1S-a** show no signs of decomposition after 6 years of storage in the solid-state under ambient conditions. Derivatives of **1O-a** also exhibit long-term stability in the solid-state.

Precursors **2** were tested for photostability and photochemical formation of the corresponding radicals **1**. The results demonstrated that all precursors **2** were stable under ambient conditions, while photocyclization of **2O-a**–**2O-c** in CH_2Cl_2 solutions gave complex reaction mixtures from which **1O-a** and **1O-c** were isolated in 7% and 5% yield, respectively. As expected, attempts at the photocyclization of 8-(2-nitrophenylsulfanyl)-3-phenylbenzo[*e*][1,2,4]triazine (**3S**) did not yield the desired radical **1S-a** and most of the substrate was recovered. This is in sharp contrast to a moderately efficient photocyclization of the analogous oxygen derivative **3O** to form **1O-a** (31% yield) under the same conditions.[32]

The requisite precursors **2O** and **2S** were obtained from 8-fluoro-3-phenylbenzo[*e*][1,2,4]triazine[27] (**4**) by nucleophilic aromatic substitution reactions with the appropriate *ortho*-

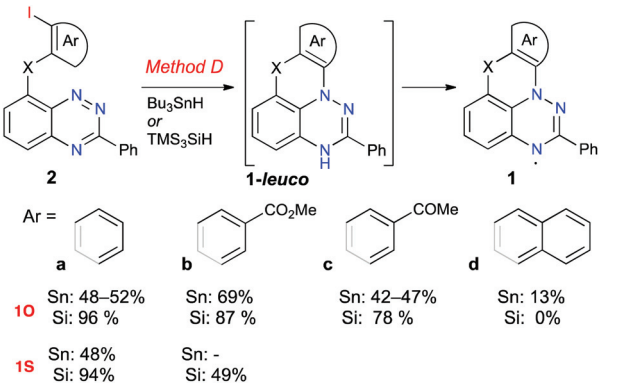

Fig. 2 Cyclization of benzo[e][1,2,4]triazines **2** to radicals **1**. Reagents and conditions, Method D: 1. Bu_3SnH or TMS_3SiH, AIBN, toluene, 80 °C, 4 h 2. Air.

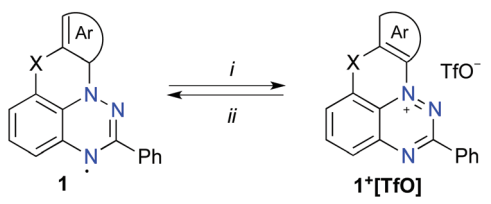

Scheme 1 Interconversion of cations $\mathbf{1}^+$ and radicals **1**. Reagents and conditions: (i) AgOTf, CH_2Cl_2/CH_3CN (9 : 1), 50 °C, 5–10 min (ii) 1. Zn powder, AcOH, CH_2Cl_2/CH_3CN (9 : 1), 50 °C, 5 min; 2. Air.

iodo phenols **5O** (X = O) or thiols **5S** (X = S) in the presence of NaH (Scheme 2).

The iodoarenes **5O** and **5S-a** were obtained using modified literature procedures by iodination of the appropriate phenols and diazotization of 2-iodoaniline, respectively.[51] Iodomercaptan **5S-b** was obtained from methyl 4-amino-3-iodobenzoate as shown in Scheme 3. Thus, treatment of 4-aminobenzoate **6** with pyridine iodine monochloride in MeOH gave methyl 4-amino-2-iodobenzoate (**7**) in 85% yield.[52] To avoid the double iodination of **6** and to obtain high yields of **7**, the reaction mixture was quenched with $Na_2S_2O_3$ before the workup. The ester **7** was diazotized and then treated with EtOCSSK, subsequently with KOH/EtOH and finally with iodine. The resulting 4,4′-disulfanediylbis(3-iodobenzoic acid) (**8**) was partially purified and transformed to dimethyl ester **9** with diazomethane in THF. Finally, the disulfide **9** was reduced with $NaBH_4$ in THF/MeOH according to a general literature procedure,[53] giving methyl 3-iodo-4-mercaptobenzoate (**5S-b**).

Mechanistic considerations

The observed successful formation of **1-*leuco*** in a radical chain process indicates that (a) the addition of the transient radical **10** to the N(1) atom is favorable and fast, and (b) the resulting radical **1** efficiently transfers an H atom from the donor R_3E–H (E = Sn or Si, Fig. 3). DFT calculations at the B3LYP/6-31G(2d,p) level of theory performed in benzene dielectric medium indeed show a low barrier to the N(1) addition of radical **10O-a** ($\Delta G^{\ddagger}_{298}$ = 3.1 kcal mol^{-1}) and high exotherm for the formation of **1O-a** (ΔH = −55.3 kcal mol^{-1}, Fig. 3). More importantly, the H transfer takes place in spite of the relatively low N–H bond dissociation energy (BDE) in **1-*leuco***, calculated to be about 69 kcal mol^{-1},[30] which compares to the experimental BDE of 73.4 ± 2 kcal mol^{-1} for Bu_3SnH in benzene.[54]

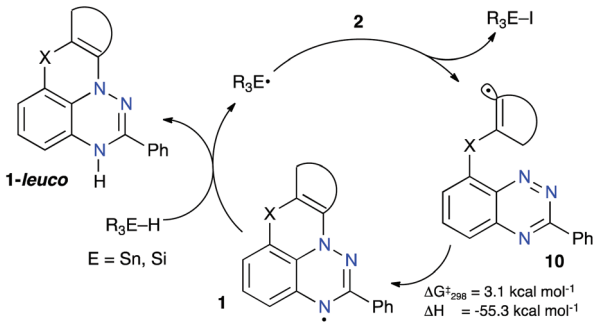

Fig. 3 Proposed mechanism for the formation of **1-*leuco*** in a radical chain process and DFT-derived thermochemical parameters for the N-addition step in **10O-a**.

Crystal and molecular structures

The structure of 10-acetyl derivative **1O-c** was confirmed with a single-crystal XRD analysis (Fig. 4 and the ESI†). The analysis revealed that **1O-c** crystallizes in the triclinic space group $P\bar{1}$. The asymmetric unit of **1O-c** contains two molecules, for which the dimensions of the heterocyclic skeleton are consistent with those found in similar systems.[27,29,30] The data showed that the heterocyclic core is nearly ideally planar. The C(2)–Ph ring is twisted from the coplanar orientation with the heterocycle by 4.2° and 5.3° in the two symmetry-independent molecules. The supramolecular system of **1O-c** consists of two types of slipped stacks extending along the [1 0 0] direction. Each stack is formed by symmetry-equivalent molecules with an interplanar separation of 3.183 Å (for stack A) and 3.246 Å (for stack B) and slippage angles of 27.0° (for stack A) and 62.2° (for stack B). Stacks A are stabilized by C(2)···C(7a) close contacts of 3.228 Å.

Electronic spectroscopy and electrochemistry

The electronic properties of the new radicals **1O-c** and **1S-b** were analyzed using spectroscopic (UV–vis and EPR) and

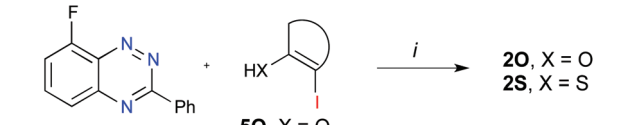

Scheme 2 Synthesis of derivatives **2O** and **2S**. Reagents and conditions: (i) iodoarene **5**, 60% NaH, DMSO, 80 °C, 6 h.

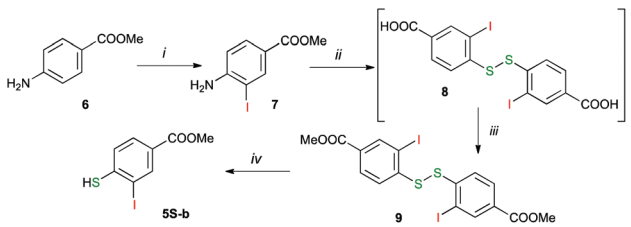

Scheme 3 Synthesis of mercaptan **5S-b**. Reagents and conditions: (i) 1. pyridine iodine monochloride, MeOH, rt, 2 h; 2. $Na_2S_2O_3$; 85% yield; (ii) 1. $NaNO_2$, aq HCl, ice bath; 2. EtOCSSK; 3. KOH, EtOH, reflux, 10 h; 4. I_2, H_2O; 40–56% yield, crude; (iii) CH_2N_2, THF/Et_2O, 0 °C, 10 min; 70–72% yield; (iv) $NaBH_4$, THF/MeOH, quant.

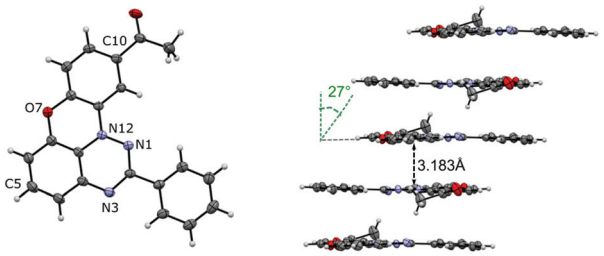

Fig. 4 A displacement ellipsoid diagram for molecule A of **1O-c** and slipped stack A indicating the distances between the average planes and the slippage angle. Ellipsoids are set at the 50% probability level and labelled according to the chemical structure. Selected intramolecular dimensions: N(1)–N(12), 1.360(1) Å; N(12)–C(11a), 1.399(1) Å; C(10)–Ac, 1.496(2) Å. For molecule B and other details, see the ESI.†

electrochemical methods. Data revealed that both radicals exhibit typical strong absorption in the UV region and broad, low-intensity absorption bands in the entire visible range. The absorption bands of sulfur analogues **1S-a** and **1S-b** are bathochromically shifted relative to those of the oxygen analogues and exhibit absorption maxima at about 680 nm and 755 (sh) nm (Fig. 5). Analysis of the spectra demonstrated that the optical band gaps, as determined from the absorption edge, are typically about 1.7 eV for radicals **1O-a–1O-d**, while those of the sulfur analogs **1S-a** and **1S-b** are markedly lower at about 1.5 eV (Table 1).

Cyclic voltammetry revealed that the oxidation and reduction processes are quasi-reversible for all derivatives (Fig. 5, Table 1). The oxidation potentials $E_{1/2}{}^{0/+1}$ in the "oxo" series increase slightly from −0.15 V for the parent **1O-a** to −0.09 V for **1O-b** and to −0.075 V for the 10-acetyl derivative **1O-c**. Similarly, the reduction potentials $E_{1/2}{}^{-1/0}$ increase for C(10)–substituted derivatives **1O-b** and **1O-c**. This effect was recently correlated with the σ_m substituent parameter for a larger pool of **1O** derivatives.[30] Analysis of the pair of **1S** derivatives reveals the same trend: there is an anodic shift of redox potentials upon substitution of the parent with the COOMe group (Table 1). Incidentally, the magnitude of this shift in $E_{1/2}{}^{0/+1}$ is exactly 0.065 eV in both pairs of radicals, while the reduction potential is affected more strongly in the sulfur pair ($\Delta E_{1/2}{}^{-1/0}$ = 0.059 V for the **1O** pair and 0.099 V for the **1S** pair).

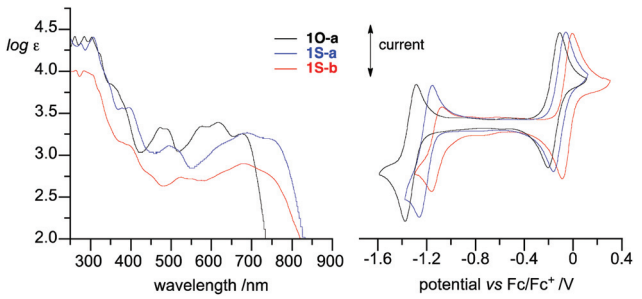

Fig. 5 Left: UV/vis spectra in CH_2Cl_2 and right: Cyclic voltammograms (0.5 mM in CH_2Cl_2 [*n*-Bu_4N]$^+PF_6^-$ (50 mM), at ~20 °C, 50 mV s^{-1}, glassy carbon working electrode) for radicals **1O-a** (black), **1S-a** (blue), and **1S-b** (red).

Table 1 Electrochemical data for planar Blatter radical derivatives **1**

	Radical R	$E_{1/2}{}^{-1/0}$ [a]/V	$E_{1/2}{}^{0/+1}$ [a]/V	E_{cell} [b]/V	E_g [c]/eV
O-a	H[d]	−1.317	−0.154	1.163	1.66
O-b	COOMe[d]	−1.258	−0.089	1.169	1.72
O-c	Ac	−1.222	−0.075	1.147	1.68
O-d	Naphth[e]	−1.354	−0.212	1.142	1.67
S-a	H	−1.202	−0.112	1.090	1.48
S-b	COOMe	−1.103	−0.047	1.056	1.51

[a] Potentials *vs.* Fc/Fc^+. [b] $E_{cell} = E_{1/2}{}^{0/+1} - E_{1/2}{}^{-1/0}$. [c] Optical band gap from the absorption edge. [d] Ref. 28. [e] Ref. 32. For details, see the ESI.†

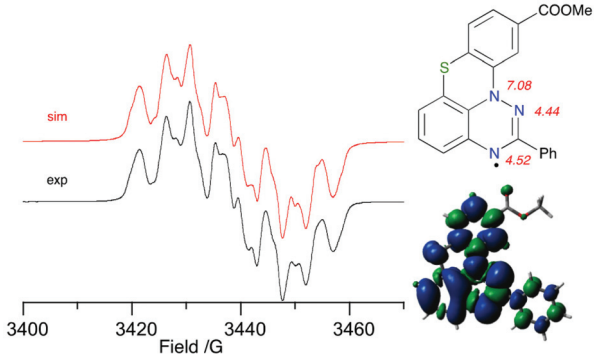

Fig. 6 Left: experimental (black) and simulated (red) EPR spectra for **1S-b** recorded in benzene at *ca.* 20 °C. Right: assignment of the resulting hfcc and total spin density in **1S-b**. Contour values are plotted at ±0.02 (e per bohr^3)$^{1/2}$.

EPR spectroscopy

Electron paramagnetic spectroscopy (EPR) revealed that the experimental hyperfine coupling constants (hfcc) a_N for **1O-c** and **1S-b** (Fig. 6) are consistent with those for other planar benzo[*e*][1,2,4]triazinyl radicals.[30] Analysis of the results indicates that the $a_{N(12)}$ value slightly decreases (from 7.42 G for **1S-a** to 7.08 G for **1S-b**), while the values for $a_{N(1)}$ and $a_{N(3)}$ increase, *e.g.* for $a_{N(1)}$, from 4.38 G for **1S-a** to 4.52 G for **1S-b**. This substituent effect is consistent with that observed in the oxygen analogues **1O**.[30]

Conclusions

We have demonstrated a new and efficient method for the formation of planar Blatter radical derivatives through Bu_3SnH- and TMS_3SiH-assisted cyclization of aryl iodides. Unlike in previous such reactions, the cyclization takes place at the heterocyclic N atom. The new method complements the existing methods A–C for the preparation of planar Blatter radicals with important advantages. Similarly to the Pschorr-type cyclization (Method B), it tolerates functional groups, such as COOMe and COMe, and allows for obtaining the desired products with significantly higher yields (Table 2). Most importantly, for the first time, it permits the preparation of functio-

Table 2 Comparison of Methods A–D in the formation of radicals **1**

Radical		Method				
1	R	A	B	C	D-Sn	D-Si
O-a	H	20–25%	57–64%	7–64%	48–52%	96%
O-b	COOMe	[a,b]	48–55%	[b]	69%	87%
O-c	Ac	[a,b]	[b]	5%	42–47%	78%
O-d	[c]	0%	0%	14–55%	(13%)[d]	0%
S-a	H	22–30%	[a,b]	[a]	48%	94%
S-b	COOMe	[a,b]	[a,b]	0%	[b]	49%

[a] Not compatible. [b] Not attempted. For references see the text. [c] Naphtho-fused radical. [d] Low stability on isolation.

nalized derivatives of the [1,2,4]triazino[5,6,1-*kl*]phenothiazinyl (radical **1S-b**), which was not possible through other methods. This discovery opens up possibilities for further exploration of functionalized [1,2,4]triazino[5,6,1-*kl*]phenothiazinyl radicals, especially of their magnetic properties in the solid state. This work is underway in our laboratory.

The radical cyclization of aryl iodides method also gives the ring-extended derivatives, such as the naphtho-derivative **1O-d**, but in this case, the photocyclization Method C appears to be more efficient. The newly discovered Method D for obtaining radicals **1** makes a significant contribution to the development of new materials for molecular electronics, spintronics, and functional self-organizing materials.

Computational details

Quantum-mechanical calculations were carried out using the Gaussian 09 suite of programs.[55] Geometry optimizations were undertaken at the UB3LYP/6-31G(2d,p) level of theory using tight convergence limits and appropriate symmetry constraints. The transition state for the cyclization of **10O-a** was located with the QST3 keyword. Calculations involving the cyclization of radical **10O-a** to form **1O-a** used SCF energies for reaction components in benzene dielectric medium requested with the SCRF(Solvent = Benzene) keyword (PCM model;[56] single point calculations at the UB3LYP/6-311++G(2d,p)// UB3LYP/6-31G(2d,p) level of theory) and thermodynamic corrections obtained with the UB3LYP/6-31G(2d,p) method.

Isotropic Fermi contact coupling constants for radical **1S-b** were calculated using the UCAM-B3LYP/gen //UB3LYP/6-31G (2d,p) method in benzene dielectric medium requested with the SCRF(Solvent = Benzene) keyword (PCM model[56]). The basis set was requested with the GEN keyword: EPRIII basis for all light elements and 6-311 + G(2df) for the S atom.

Experimental section

General

Reagents and solvents were obtained commercially. Heat for reactions requiring elevated temperatures was supplied using oil baths. NMR spectra were obtained at 600 MHz (^{1}H) and 151 MHz (^{13}C) in $CDCl_3$ and referenced to the solvent (δ = 7.26 ppm for ^{1}H and δ = 77.16 ppm for ^{13}C) or in DMSO-d_6 and referenced to the solvent (δ = 2.50 ppm for ^{1}H and δ = 39.52 ppm for ^{13}C).[57] IR spectra were recorded using a Nexus FT-IR Thermo Nikolet IR spectrometer in KBr tablets. UV spectra were measured in CH_2Cl_2 using a PerkinElmer Lambda 45 spectrophotometer. Melting points were determined using a Stuart SMP30 Advanced Digital Melting Point Apparatus and are uncorrected. High-resolution mass spectrometry (HRMS) measurements were performed using SYNAPT G2-Si High Definition Mass Spectrometry equipped with an ESI or APCI source and Quantitative Time-of-Flight (QuanTof) mass analyzer. Other mass spectrometry measurements were performed using a Varian 500-MS LC Ion Trap Spectrometer. In all cases little or no fragmentation was observed, and the M, [M + H] or [M − H] peaks were the most intense signals.

Et_3N-passivated SiO_2 gel and chromatographic separation of radicals 1. The solid support was mixed with a 2% solution of Et_3N in CH_2Cl_2 and the solvent was evaporated to dryness (rotavap). For the chromatographic separation of radicals, small amounts of dry, passivated SiO_2 were added to the reaction mixture, and the resulting mixture was evaporated to dryness <50 °C. The resulting solid was deposited onto a passivated SiO_2 plug or column (pet. ether), and the product was eluted with a CH_2Cl_2/pet. ether mixture.

The activity and effectiveness of the solid supports varied between suppliers and even between batches, and the exact conditions for isolation of the radicals required adjustments for each new container.

General procedure for Method D-Sn. Bu_3SnH-assisted cyclization of aryl iodides 2

To a solution of aryl iodide **2** (0.25 mmol) in dry toluene (4 mL), Bu_3SnH (0.50 mmol) was added and stirred at 80 °C under an atmosphere of Ar. Then, AIBN (0.15 mmol) dissolved in dry toluene (2 mL) was added to the reaction mixture over a period of 4 h using a syringe pump. After 4 h the reaction mixture was cooled and the solvent was evaporated to dryness. The residue was re-dissolved in ethyl acetate (20 mL), saturated aqueous potassium fluoride (20 mL) was added, and the mixture was stirred vigorously for 15 min. The organic fraction was separated, washed with brine (2 × 30 mL), dried (Na_2SO_4), and concentrated *in vacuo.* The crude product was separated using a short silica gel column passivated with Et_3N (*vide supra*). To remove organotin impurities, the radical was oxidized to form the triflate salt **1$^+$**, purified, and subsequently reduced back to radical **1**.

Formation of salts 1$^+$[OTf] by oxidation of radicals 1. Radical **1** was dissolved in CH_2Cl_2/CH_3CN (9 : 1) and AgOTf (0.30 mmol, 1.2 eq.) was added in one portion. The reaction mixture was stirred for 5–10 minutes at 50 °C until the substrate was no longer detectable by TLC (pet. ether/AcOEt, 9 : 1). The crude salt was purified using a short silica gel column with CH_2Cl_2/MeOH 9 : 1 as the eluent.

Formation of 1 by reduction of salts 1$^+$[OTf]. Salt **1$^+$[OTf]** was dissolved in a 9 : 1 CH_2Cl_2/CH_3CN mixture (25 mL), and 100 μL of AcOH and 150 mg of zinc powder were added. The reaction mixture was stirred at 50 °C for 5 min until the starting salt **1$^+$[OTf]** was no longer detectable by TLC analysis (pet. ether/AcOEt, 9 : 1). The reaction mixture was cooled, filtered through Celite, washed with H_2O (2 × 30 mL), dried (Na_2SO_4), and concentrated *in vacuo.* The resulting product was recrystallized by slow evaporation of a CH_2Cl_2/cyclohexane solution.

General procedure for Method D-Si. TMS_3SiH-assisted cyclization of aryl iodides 2

To a solution of aryl iodide **2** (0.25 mmol) in dry toluene (4 mL), TMS_3SiH (0.50 mmol) was added, and the solution was stirred at 80 °C under an atmosphere of Ar. Then, AIBN (0.15 mmol) dissolved in dry toluene (2 mL) was added to the

reaction mixture over a period of 4 h using a syringe pump. After 4 h, the reaction mixture was cooled, and the solvent was evaporated to dryness. The crude product was absorbed on passivated SiO_2 (*vide supra*), and radical **1** was isolated using a short silica gel column with passivated SiO_2. The product was washed with warm cyclohexane (3×) and recrystallized from CH_3CN.

2-Phenyl-3*H*-[1,2,4]triazino[5,6,1-*kl*]phenoxazin-3-yl (1O-a).[27,28] Method D-Sn: 48–52% yield, Method D-Si: 96% yield; eluent: pet. ether/AcOEt, 95 : 5; blue-gray crystals. Analytical data identical to those previously reported.[27] HRMS (ESI-TOF) *m*/*z* $[M + H]^+$ calcd for $C_{19}H_{13}N_3O$: 299.1059; found: 299.1055.

10-Methoxycarbonyl-2-phenyl-3*H*-[1,2,4]triazino[5,6,1-*kl*]-phenoxazin-3-yl (1O-b).[27] Method D-Sn: 69% yield, Method D–Si: 87% yield; eluent: pet. ether/AcOEt, 95 : 5; blue-gray crystals. Analytical data identical to the previously reported.[28] HRMS (ESI-TOF) *m*/*z* $[M + H]^+$ calcd for $C_{21}H_{15}N_3O_3$: 357.1113; found: 357.1120.

10-Acetyl-2-phenyl-3*H*-[1,2,4]triazino[5,6,1-*kl*]phenoxazin-3-yl (1O-c). Method D-Sn: 42–47% yield, Method D-Si: 78% yield; eluent: pet. ether/AcOEt, 9 : 1; blue-green crystals: mp 187–188 °C (MeCN); IR (KBr) ν 1680, 1567, 1383, 1348, 1266, 1210, 1162, 1031, 791, 696 cm^{-1}; UV (CH_2Cl_2) λ_{max} ($\log \varepsilon$) 280 (3.58), 315 (4.24), 377 (3.64), 431 (3.29), 514.5 (3.19), 570 (3.18), 618 (3.24), 673 (3.13) nm; HRMS (ESI-TOF) $[M + H]^+$ *m*/*z* calcd for $C_{21}H_{15}N_3O_2$: 341.1164; found: 341.1166. Anal. Calcd for $(C_{21}H_{14}N_3O_2)_3 \cdot H_2O$: C, 72.82; H, 4.27; N, 12.13. Found: C, 72.99; H, 4.23; N, 12.42.

2-Phenyl-3*H*-benzo[*a*][1,2,4]triazino[5,6,1-*kl*]phenoxazin-3-yl (1O-d).[32] Method D-Sn: 13% yield (without salt formation), Method-Si: 0% yield; eluent: pet. ether/AcOEt, 95 : 5; blue-gray crystals. Analytical data identical to those previously reported.[32] HRMS (ESI-TOF) $[M + H]^+$ *m*/*z* calcd for $C_{23}H_{15}N_3O$: 349.1215; found: 349.1222.

2-Phenyl-3*H*-[1,2,4]triazino[5,6,1-*kl*]phenothiazine-3-yl (1S-a).[27] Method D-Sn: 48% yield, Method D-Si: 94% yield; eluent: pet. ether/AcOEt, 9 : 1 blue-green crystals. Analytical data identical to those previously reported.[27] HRMS (ESI-TOF) $[M + H]^+$ *m*/*z* calcd for $C_{19}H_{13}N_3S$: 315.0830; found: 315.0836.

10 methoxycarbonyl-2-phenyl-3*H*-[1,2,4]triazino[5,6,1-*kl*]phenothiazin-3-yl (1S-b). Method D-Si: 49% yield; eluent: pet. ether/AcOEt, 9 : 1; blue-green crystals: mp 185–186 °C (MeCN); IR (KBr) ν 2956, 2925, 2854, 1728, 1470, 1436, 1404, 1249, 1080, 1013, 844, 754, 688 cm^{-1}; UV (CH_2Cl_2) λ_{max} ($\log \varepsilon$) 263 (4.02), 284 (4.02), 399 (3.12 sh), 524 (2.74), 679 (2.90), 746 (2.75 sh) nm; HRMS (ESI-TOF) $[M + H]^+$ *m*/*z* calcd for $C_{21}H_{15}N_3O_2S$: 373.0898; found: 373.0892. Anal. Calcd for $C_{21}H_{14}N_3O_2S$: C, 67.73; H, 3.79; N, 11.28. Found: C, 67.68; H, 3.93; N, 11.25.

Synthesis of iodoarenes 2. General procedure

To a stirred solution of phenol **5O** or thiophenol **5S** (1.10 mmol) dissolved in DMSO (4 mL), 60% NaH (45 mg, 1.10 mmol) was added in one portion. After 15 min of stirring, 8-fluoro-3-phenylbenzo[*e*][1,2,4]triazine[27] (**4**, 225.2 mg, 1.00 mmol) was added, and the reaction was stirred under Ar at 80 °C for 6 h. After cooling, CH_2Cl_2 (30 mL) was added, and the organic layer was washed well with water (3 × 25 mL) and brine (25 mL). The combined organic extracts were dried (Na_2SO_4), and the solvent was evaporated. The resulting solid residue was adsorbed onto passivated silica and purified by column chromatography (passivated silica). The solvent was evaporated, and the product was recrystallized from MeCN.

8-(2-Iodophenoxy)-3-phenylbenzo[*e*][1,2,4]triazine (2O-a). 368–400 mg (87–94% yield) of **2O-a** was obtained as yellow crystals: mp 138–139 °C (MeCN); ^1H NMR (600 MHz, $CDCl_3$) δ 8.82–8.76 (m, 2H), 7.96 (dd, J_1 = 8.0 Hz, J_2 = 1.5 Hz, 1H), 7.83–7.79 (m, 2H), 7.63–7.58 (m, 3H), 7.42 (dt, J_1 = 7.7 Hz, J_2 = 1.5 Hz, 1H), 7.18 (dd, J_1 = 8.0 Hz, J_2 = 1.3 Hz, 1H), 7.03 (dt, J_1 = 7.7 Hz, J_2 = 1.3 Hz, 1H), 6.89 (dd, J_1 = 6.2 Hz, J_2 = 2.7 Hz, 1H); $^{13}C\{^1H\}$ NMR (151 MHz, $CDCl_3$) δ 160.3, 155.6, 154.2, 142.3, 140.5, 139.8, 135.8, 135.6, 131.8, 130.2, 129.15, 129.10, 127.2, 123.2, 121.6, 113.8, 89.9; IR (KBr) ν 3053, 1615, 1561, 1500, 1470, 1436, 1388, 1325, 1259, 1215, 1170, 1086, 1020, 793, 759, 691 cm^{-1}; HRMS (ESI-TOF) $[M + H]^+$ *m*/*z* calcd for $C_{19}H_{13}IN_3O$: 426.0103; found: 426.0111. Anal. Calcd for $C_{19}H_{12}IN_3O$: C, 53.67; H, 2.84; N, 9.88. Found: C, 53.67; H, 2.88; N, 10.06.

8-(2-Iodo-3-methoxycarbonylphenoxy)-3-phenylbenzo[*e*][1,2,4]triazine (2O-b). 271 mg (56% yield) of **2O-b** was obtained as yellow crystals: mp 187–188 °C (MeCN); ^1H NMR (600 MHz, $CDCl_3$) δ 8.80–8.72 (m, 2H), 8.62 (d, J = 2.0 Hz, 1H), 7.97 (dd, J_1 = 8.5 Hz, J_2 = 2.0 Hz, 1H), 7.92–7.86 (m, 2H), 7.60–7.57 (m, 3H), 7.16 (dd, J_1 = 6.6 Hz, J_2 = 2.0 Hz, 1H), 6.94 (d, J = 8.7 Hz), 3.92 (s, 3H); $^{13}C\{^1H\}$ NMR (151 MHz, $CDCl_3$) δ 165.2, 160.4, 160.3, 152.6, 142.4, 141.9, 139.8, 135.7, 131.9, 131.6, 129.15, 129.10, 127.9, 125.0, 118.7, 116.8, 87.9, 52.5; IR (KBr) ν 1720, 1561, 1504, 1043, 1384, 1280, 1251, 1107, 1084, 790, 701 cm^{-1}; HRMS (ESI-TOF) $[M + H]^+$ *m*/*z* calcd for $C_{21}H_{15}IN_3O_3$: 484.0158; found: 484.0162. Anal. Calcd for $C_{21}H_{14}IN_3O_3$: C, 52.19; H, 2.92; N, 8.69. Found: C, 52.23; H, 2.85; N, 8.87.

8-(4-Acetyl-2-iodophenyloxy)-3-phenylbenzo[*e*][1,2,4]triazine (2O-c). 271 mg (58% yield) of **2O-c** was obtained as yellow crystals: mp 204–205 °C (MeCN); ^1H NMR (600 MHz, $CDCl_3$) δ 8.75–8.79 (m, 2H), 8.54 (d, J = 2.1 Hz, 1H), 7.88–7.94 (m, 3H), 7.58–7.61 (m, 3H), 7.21 (dd, J_1 = 7.1 Hz, J_2 = 1.6 Hz, 1H), 6.94 (d, J = 8.5 Hz, 1H), 2.60 (s, 3H); $^{13}C\{^1H\}$ NMR (151 MHz, $CDCl_3$) δ 195.5, 160.5, 160.3, 152.4, 142.4, 140.9, 139.7, 135.6, 135.2, 134.8, 131.9, 130.2, 129.1, 129.0, 125.2, 118.5, 117.1, 88.2, 26.6; IR (KBr) ν 1686, 1560, 1505, 1386, 1347, 1324, 1244, 1073, 847, 796, 704 cm^{-1}; HRMS (ESI-TOF) $[M + H]^+$ *m*/*z* calcd for $C_{21}H_{15}IN_3O_2$: 468.0209; found: 468.0210. Anal. Calcd for $C_{21}H_{14}IN_3O_2$: C, 53.98; H, 3.02; N, 8.99. Found: C, 53.79; H, 3.05; N, 9.05.

8-((1-Iodonaphthalen-2-yl)oxy)-3-phenylbenzo[*e*][1,2,4]triazine (2O-d). 314 mg (66% yield) of **2O-d** was obtained as yellow crystals: mp 204–206 °C (MeCN); ^1H NMR (600 MHz, $CDCl_3$) δ 8.83–8.79 (m, 2H), 8.26 (d, J = 8.5 Hz, 1H), 7.91 (d, J = 8.7 Hz, 1H), 7.85 (d, J = 8.2 Hz, 1H), 7.80–7.74 (m, 2H), 7.65 (t, J = 7.7 Hz, 1H), 7.62–7.59 (m, 3H), 7.56 (t, J = 7.6 Hz, 1H), 7.36 (d, J = 8.7 Hz, 1H), 6.85 (d, J = 7.2 Hz, 1H); $^{13}C\{^1H\}$ NMR (151 MHz, $CDCl_3$) δ 160.3, 154.3, 153.7, 142.3, 139.8, 135.9, 135.8, 135.6, 132.2, 131.9, 131.8, 131.2, 129.1, 129.0, 128.65, 128.60, 126.5, 122.9, 120.5, 113.4, 94.0; IR (KBr) ν 1610, 1558, 1504, 1440,

1384, 1347, 1323, 1246, 1220, 1086, 819, 789, 701 cm^{-1}; HRMS (ESI-TOF) $[M + H]^+$ *m*/*z* calcd for $C_{23}H_{15}IN_3O$: 476.0260; found: 476.0268. Anal. Calcd for $C_{23}H_{14}IN_3O$: C, 58.12; H, 2.97; N, 8.84. Found: C, 58.11; H, 2.93; N, 9.08.

8-((2-Iodophenyl)thio)-3-phenylbenzo[*e*][1,2,4]triazine (2S-a). 419 mg (95% yield) of **2S-a** was obtained as yellow crystals: mp 157–159 °C (MeCN); ^1H NMR (600 MHz, $CDCl_3$) δ 8.80–8.75 (m, 2H), 8.10 (dd, J_1 = 7.9 Hz, J_2 = 0.9 Hz, 1H), 7.83–7.78 (m, 2H), 7.71 (t, J = 7.9 Hz, 1H), 7.62–7.58 (m, 3H), 7.47 (dd, J_1 = 7.6 Hz, J_2 = 1.1 Hz, 1H), 7.17 (dt, J_1 = 7.8 Hz, J_2 = 1.2 Hz, 1H), 6.90 (dd, J_1 = 7.2 Hz, J_2 = 0.8 Hz, 1H); $^{13}C\{^1H\}$ NMR (151 MHz, $CDCl_3$) δ 160.6, 143.8, 142.2, 141.15, 141.10, 137.0, 136.1, 135.7, 135.6, 131.8, 131.2, 129.9, 129.1, 129.0, 125.8, 125.4, 108.6; IR (KBr) ν 1548, 1504, 1443, 1418, 1379, 1321, 1279, 1212, 1173, 1109, 1018, 981, 793, 752, 700 cm^{-1}; HRMS (ESI-TOF) $[M + H]^+$ *m*/*z* calcd for $C_{19}H_{13}IN_3S$: 441.9875; found: 441.9881. Anal. Calcd for $C_{19}H_{12}IN_3S$: C, 51.71; H, 2.74; N, 9.52; S, 7.26. Found: C, 51.64; H, 2.95; N, 9.49; S, 7.06.

8-(3-Iodo-4-methoxycarbonylphylsulfanyl)-3-phenylbenzo[*e*]-[1,2,4]triazine (2S-b). 179 mg (36% yield) of **2S-b** was obtained as yellow crystals: mp 207–208 °C (MeCN); ^1H NMR (600 MHz, $CDCl_3$) δ 8.79–8.75 (m, 2H), 8.64 (d, J = 1.7 Hz, 1H), 7.98–7.95 (m, 2H), 7.81 (q, J = 8.3 Hz, 1H), 7.62–7.58 (m, 3H), 7.49 (d, J = 8.1 Hz, 1H), 7.27 (d, J = 0.8 Hz, 1H), 3.94 (s, 3H); $^{13}C\{^1H\}$ NMR (151 MHz, $CDCl_3$) δ 165.2, 160.7, 144.3, 144.0, 142.4, 141.4, 138.4, 135.7, 135.4, 133.7, 132.0, 131.3, 130.2, 129.3, 129.2, 127.7, 104.2, 52.7; IR (KBr) ν 1715, 1546, 1503, 1432, 1367, 1277, 1236, 1111, 1018, 794, 765, 704 cm^{-1}; HRMS (ESI-TOF) $[M + H]^+$ *m*/*z* calcd for $C_{21}H_{15}IN_3O_2S$: 499.9930; found: 499.9933. Anal. Calcd for $C_{21}H_{14}IN_3O_2S$: C, 50.51; H, 2.83; N, 8.42; S, 6.42. Found C, 50.33; H, 2.68; N, 8.68; S, 6.13.

8-((2-Nitrophenyl)thio)-3-phenylbenzo[*e*][1,2,4]triazine (3S). Derivative **3S** was obtained in 76% yield (272 mg) from **4** and 2-nitrothiophenol[51] as described for **2**; yellow crystals: mp 211–212 °C (MeCN); ^1H NMR (600 MHz, $CDCl_3$) δ 8.77–8.73 (m, 2H), 8.26–8.23 (m, 1H), 8.19 (dd, J_1 = 6.4 Hz, J_2 = 3.4 Hz, 1H), 8.00–7.98 (m, 1H), 7.98 (d, J = 3.1 Hz, 1H), 7.60–7.57 (m, 3H), 7.32–7.28 (m, 2H), 6.94–6.90 (m, 1H); $^{13}C\{^1H\}$ NMR (151 MHz, $CDCl_3$) δ 160.5, 147.0, 154.4, 142.6, 136.3, 135.8, 135.7, 135.1, 134.6, 133.5, 132.1, 131.3, 130.8, 129.2, 129.1, 126.6, 126.0; IR (KBr) ν 1591, 1547, 1508, 1451, 1336, 1304, 1252, 1105, 1018, 839, 783, 140, 699 cm^{-1}; HRMS (ESI-TOF) $[M + Na]^+$ *m*/*z* calcd for $C_{19}H_{12}N_4O_2NaS$: 383.0579; found: 383.0565. Anal. Calcd for $C_{19}H_{12}N_4O_2S$: C, 63.32; H, 3.36; N, 15.55; S, 8.90. Found: C, 63.16; H, 3.34; N, 15.42; S, 8.76.

Synthesis of methyl-3-iodo-4-mercaptobenzoate (5S-b)

4,4′-Disulfanediylbis(3-iodobenzoic acid) (8). A suspension of $NaNO_2$ (70.4 mg, 1 mmol) in water (500 μL) was added over 10 min to an ice-cooled solution of methyl 4-amino-2-iodobenzoate[51] (7, 277 mg, 1.0 mmol) in 35% aqueous HCl (167 μL, 0.02 mol) containing ice (2.0 g). After 45 min of stirring, 20% aqueous solution of sodium acetate was added until the pH of the solution was 4–5. Next, potassium methyl xanthate[58] (146 mg, 1 mmol) in water (1 mL) was added. The reaction mixture was slowly warmed to room temperature, and the resulting mixture was dissolved in CH_2Cl_2. The organic phase was separated, dried over $MgSO_4$, and evaporated to dryness *in vacuo*. The residue was refluxed with KOH (3.0 g, 85%, 0.046 mol) in absolute ethanol (10 mL) for 10 h. The solvent was removed, the resulting mixture was dissolved in H_2O, and small amounts of I_2 were added until a permanent color change occurred. Then, the reaction mixture was acidified with HCl and the crude product precipitated. After filtration, the product was purified by crystallization with MeOH/H_2O (9 : 1) giving 111–156 mg (40–56% yield) of disulfide **8** as a pale solid: mp > 230 °C (MeOH/H_2O, 9 : 1); ^1H NMR (600 MHz, DMSO-d_6) δ 13.27 (s, 1H), 8.33 (s, 1H), 7.96 (dd, J_1 = 8.3 Hz, J_2 = 1.7 Hz, 1H), 7.50 (d, J = 8.3 Hz, 1H); IR (KBr) ν 1690, 1580, 1542, 1412, 1369, 1296, 1244, 759 cm^{-1}; HRMS (ESI-TOF) $[M - H]^-$ *m*/*z* calcd for $C_{14}H_{14}I_2O_4S_2$: 556.7875; found: 556.7883. Anal. Calcd for $C_{14}H_8I_2O_4S_2$: C, 30.13; H, 1.44. Found: C, 30.32; H, 1.57.

The acid was used in the next step without further purification.

Dimethyl 4,4′-disulfanediylbis(3-iodobenzoate) (9). To a solution of 4,4′-disulfanediylbis(3-iodobenzoic acid) (**8**, 140 mg, 0.25 mmol) in THF (3 mL), a solution of CH_2N_2 (3 eq., freshly prepared from 77 mg of *N*-methyl-*N*-nitrosourea) in diethyl ether was added at 0 °C, and the reaction mixture was stirred for 10 min. The solvent was removed, and the crude product was purified by column chromatography using silica gel (hexane/ethyl acetate = 9 : 1) giving 103–106 mg (70–72% yield) dimethyl ester **9** as white crystals: mp 180–181 °C (AcOEt); ^1H NMR (600 MHz, $CDCl_3$) δ 8.45 (d, J = 1.7 Hz, 1H), 7.95 (dd, J_1 = 8.3 Hz, J_2 = 1.8 Hz, 1H), 7.47 (d, J = 8.3 Hz, 1H), 3.90 (s, 3H); $^{13}C\{^1H\}$ NMR (151 MHz, $CDCl_3$) δ 165.2, 144.9, 140.5, 130.1, 130.0, 125.6, 94.2, 52.6; IR (KBr) ν 1721, 1578, 1544, 1429, 1366, 1286, 1235, 1114, 1014, 832, 758 cm^{-1}; HRMS (ESI-TOF) $[M + H]^+$ *m*/*z* calcd for $C_{16}H_{13}I_2O_4S_2$: 586.8345; found: 586.8344. Anal. Calcd for $C_{16}H_{12}I_2O_4S_2$: C, 32.78; H, 2.06; S, 10.94. Found: C, 32.79; H, 2.18; S, 11.16.

Methyl 3-iodo-4-mercaptobenzoate (5S-b). Dimethyl 4,4′-disulfanediylbis(3-iodobenzoate) (**9**) was reduced with $NaBH_4$ in THF at reflux in the presence of MeOH according to a general literature procedure[53] to give **5S-b** in essentially quant. yield, which was used for the next step without further purification: ^1H NMR (600 MHz, $CDCl_3$) δ 8.40 (d, J = 1.7 Hz, 1H), 7.82 (dd, J_1 = 8.2 Hz, J_2 = 1.7 Hz, 1H), 7.42 (d, J = 8.2 Hz, 1H), 4.35 (s, 1H), 3.88 (s, 3H); $^{13}C\{^1H\}$ NMR (151 MHz, $CDCl_3$) δ 165.3, 145.4, 140.7, 129.7, 128.2, 127.6, 96.6, 52.2; HRMS (ESI-TOF) $[M - H]^-$ *m*/*z* calcd for $C_8H_8IO_2S$: 292.9133; found: 292.9129.

Preparation of other intermediates is described in the ESI.†

Author contributions

The manuscript was written through contributions of all authors and all authors have given approval to the final version of the manuscript.

Conflicts of interest

The authors declare no competing financial interest.

Acknowledgements

Support for this work was provided by the National Science Center (2019/03/X/ST4/02006 and 2017/25/B/ST5/02851). The authors thank Dr. Paweł Tokarz for helpful discussions.

Notes and references

1 T. J. J. Muller and U. H. F. Bunz, *Functional Organic Materials*, Wiley, 2006.
2 I. Ratera and J. Veciana, Playing with organic radicals as building blocks for functional molecular materials, *Chem. Soc. Rev.*, 2012, **41**, 303–349.
3 D. A. Wilcox, V. Agarkar, S. Mukherjee and B. W. Boudouris, Stable radical materials for energy applications, *Annu. Rev. Chem. Biomol. Eng.*, 2018, **9**, 83–103.
4 Z. X. Chen, Y. Li and F. Huang, Persistent and stable organic radicals: Design, synthesis, and applications, *Chem.*, 2021, **7**, 288–332.
5 S. Mukherjee and B. W. Boudouris, *Organic Radical Polymers*, Springer International Publishing, 2017.
6 L. Ji, J. Shi, J. Wei, T. Yu and W. Huang, Air-stable organic radicals: New-generation materials for flexible electronics?, *Adv. Mater.*, 2020, **32**, 1908015.
7 J. M. Hudson, T. J. H. Hele and E. W. Evans, Efficient light-emitting diodes from organic radicals with doublet emission, *J. Appl. Phys.*, 2021, **129**, 180901.
8 M. Deumal, V. Vela, M. Fumanal, J. Ribas-Arino and J. J. Novoa, Insights into the magnetism and phase transitions of organic radical-based materials, *J. Mater. Chem. C*, 2021, **9**, 10624–10646.
9 H. M. Blatter and H. Lukaszewski, A new stable free radical, *Tetrahedron Lett.*, 1968, **9**, 2701–2705.
10 F. J. M. Rogers, P. L. Norcott and M. L. Coote, Recent advances in the chemistry of benzo[*e*][1,2,4]triazinyl radicals, *Org. Biomol. Chem.*, 2020, **18**, 8255–8277.
11 Y. Ji, L. Long and Y. Zheng, Recent advances of stable Blatter radicals: Synthesis, properties and applications, *Mater. Chem. Front.*, 2020, **4**, 3433–3443.
12 F. A. Neugebauer and I. Umminger, Über 1,4-dihydro-1,2,4-benzotriazinyl-radikale, *Chem. Ber.*, 1980, **113**, 1205–1225.
13 C. P. Constantinides, P. A. Koutentis, H. Krassos, J. M. Rawson and A. J. Tasiopoulos, Characterization and magnetic properties of a "super stable" radical 1,3-diphenyl-7-trifluoromethyl-1,4-dihydro-1,2,4-benzotriazin-4-yl, *J. Org. Chem.*, 2011, **76**, 2798–2806.
14 F. A. Neugebauer and G. Rimmler, ENDOR and triple resonance studies of 1,4-dihydro-1,2,4-benzotriazinyl radicals and 1,4-dihydro-1,2,4-benzotriazine radical cations, *Magn. Reson. Chem.*, 1988, **26**, 595–600.
15 A. A. Berezin, C. P. Constantinides, S. I. Mirallai, M. Manoli, L. L. Cao, J. M. Rawson and P. A. Koutentis, Synthesis and properties of imidazolo-fused benzotriazinyl radicals, *Org. Biomol. Chem.*, 2013, **11**, 6780–6795.
16 A. A. Berezin, G. Zissimou, C. P. Constantinides, Y. Beldjoudi, J. M. Rawson and P. A. Koutentis, Route to benzo- and pyrido-fused 1,2,4-triazinyl radicals via *N*′-(het)aryl-N′-[2-nitro(het)aryl]hydrazides, *J. Org. Chem.*, 2014, **79**, 314–327.
17 G. Karecla, P. Papagiorgis, N. Panagi, G. A. Zissimou, C. P. Constantinides, P. A. Koutentis, G. Itskos and S. C. Hayes, Emission from the stable Blatter radical, *New J. Chem.*, 2017, **41**, 8604–8613.
18 Y. Zheng, M.-s. Miao, M. C. Kemei, R. Seshadri and F. Wudl, The pyreno-triazinyl radical – magnetic and sensor properties, *Isr. J. Chem.*, 2014, **54**, 774–778.
19 Y. Zheng, M.-s. Miao, G. Dantelle, N. D. Eisenmenger, G. Wu, I. Yavuz, M. L. Chabinyc, K. N. Houk and F. Wudl, A solid-state effect responsible for an organic quintet state at room temperature and ambient pressure, *Adv. Mater.*, 2015, **27**, 1718–1723.
20 M. Jasiński, J. Szczytko, D. Pociecha, H. Monobe and P. Kaszyński, Substituent-dependent magnetic behavior of discotic benzo[*e*][1,2,4]triazinyls, *J. Am. Chem. Soc.*, 2016, **138**, 9421–9424.
21 M. Jasiński, K. Szymańska, A. Gardias, D. Pociecha, H. Monobe, J. Szczytko and P. Kaszyński, Tuning the magnetic properties of columnar benzo[*e*][1,2,4]triazin-4-yls with the molecular shape, *ChemPhysChem*, 2019, **20**, 636–644.
22 F. Ciccullo, A. Calzolari, K. Bader, P. Neugebauer, N. M. Gallagher, A. Rajca, J. van Slageren and M. B. Casu, Interfacing a potential purely organic molecular quantum bit with a real-life surface, *ACS Appl. Mater. Interfaces*, 2019, **11**, 1571–1578.
23 F. Ciccullo, N. M. Gallagher, O. Geladari, T. Chassé, A. Rajca and M. B. Casu, A derivative of the Blatter radical as a potential metal-free magnet for stable thin films and interfaces, *ACS Appl. Mater. Interfaces*, 2016, **8**, 1805–1812.
24 J. Z. Low, G. Kladnik, L. L. Patera, S. Sokolov, G. Lovat, E. Kumarasamy, J. Repp, L. M. Campos, D. Cvetko, A. Morgante and L. Venkataraman, The environment-dependent behavior of the Blatter radical at the metal–molecule interface, *Nano Lett.*, 2019, **19**, 2543–2548.
25 M. Demetriou, A. A. Berezin, P. A. Koutentis and T. Krasia-Christoforou, Benzotriazinyl-mediated controlled radical polymerization of styrene, *Polym. Int.*, 2014, **63**, 674–679.
26 J. Areephong, K. M. Mattson, N. J. Treat, S. O. Poelma, J. W. Kramer, H. A. Sprafke, A. A. Latimer, J. Read de Alaniz and C. J. Hawker, Triazine-mediated controlled radical polymerization: new unimolecular initiators, *Polym. Chem.*, 2016, **7**, 370–374.
27 P. Kaszyński, C. P. Constantinides and V. G. Young Jr., The planar Blatter radical: Structural chemistry of 1,4-dihydrobenzo[*e*][1,2,4]triazin-4-yls, *Angew. Chem., Int. Ed.*, 2016, **55**, 11149–11152.

28 P. Bartos, B. Anand, A. Pietrzak and P. Kaszyński, Functional planar Blatter radical through Pschorr-type cyclization, *Org. Lett.*, 2020, **22**, 180–184.
29 A. A. Hande, C. Darrigan, P. Bartos, P. Baylère, A. Pietrzak, P. Kaszyński and A. Chrostowska, UV-photoelectron spectroscopy of stable radicals: the electronic structure of planar Blatter radicals as materials for organic electronics, *Phys. Chem. Chem. Phys.*, 2020, **22**, 23637–23644.
30 P. Bartos, A. A. Hande, A. Pietrzak, A. Chrostowska and P. Kaszyński, Substituent effects on the electronic structure of the flat Blatter radical: Correlation analysis of experimental and computational data, *New J. Chem.*, 2021, **45**, 22876–22887.
31 K. I. Shivakumar, D. Pociecha, J. Szczytko, S. Kapuściński, H. Monobe and P. Kaszyński, Photoconductive bent-core liquid crystalline radicals with a paramagnetic polar switchable phase, *J. Mater. Chem. C*, 2020, **8**, 1083–1088.
32 P. Bartos, V. G. Young and P. Kaszyński, Ring-fused 1,4-dihydro[1,2,4]triazin-4-yls through photocyclization, *Org. Lett.*, 2020, **22**, 3835–3840.
33 M. Gurry and F. Aldabbagh, A new era for homolytic aromatic substitution: Replacing Bu_3SnH with efficient light-induced chain reactions, *Org. Biomol. Chem.*, 2016, **14**, 3849–3862.
34 A. G. Davies, Tin organometallics, *Compr. Organomet. Chem. III*, 2007, **3**, 809–883.
35 A. J. Clark, Compounds of group 14 (Ge, Sn, Pb), in *Science of Synthesis*, ed. E. J. Thomas, Thieme, Stuttgart, 2003, vol. 5, pp. 205–274.
36 C. Chatgilialoglu, C. Ferreri, Y. Landais and V. I. Timokhin, Thirty years of $(TMS)_3SiH$: A milestone in radical-based synthetic chemistry, *Chem. Rev.*, 2018, **118**, 6516–6572.
37 C. Chatgilialoglu and J. Lalevée, Recent applications of the $(TMS)_3SiH$ radical-based reagent, *Molecules*, 2012, **17**, 527–555.
38 W. R. Bowman and J. M. D. Storey, Synthesis using aromatic homolytic substitution – recent advances, *Chem. Soc. Rev.*, 2007, **36**, 1803–1822.
39 W. R. Bowman, M. O. Cloonan and S. L. Krintel, Synthesis of heterocycles by radical cyclisation, *J. Chem. Soc., Perkin Trans. 1*, 2001, 2885–2902.
40 R. K. Kawade, C. Hu, N. R. Dos Santos, N. Watson, X. Lin, K. Hanson and I. V. Alabugin, Phenalenannulations: Three-point double annulation reactions that convert benzenes into pyrenes, *Angew. Chem., Int. Ed.*, 2020, **59**, 14352–14357.
41 J. C. Estevez, M. C. Villaverde, R. J. Estevez and L. Castedo, Tributyltin(IV) hydride mediated free-radical syntheses of dehydrodibenzochromanones, dehydrodibenzocoumaranones and aristolactams, *Tetrahedron*, 1995, **51**, 4075–4082.
42 H. Takiguchi, K. Ohmori and K. Suzuki, Synthesis and determination of the absolute configuration of cavicularin by symmetrization/asymmetrization approach, *Angew. Chem., Int. Ed.*, 2013, **52**, 10472–10476.
43 D. C. Harrowven, M. I. T. Nunn and D. R. Fenwick, [5] Helicenes by tandem radical cyclisation, *Tetrahedron Lett.*, 2002, **43**, 7345–7347.
44 D. C. Harrowven, I. L. Guy and L. Nanson, Efficient phenanthrene, helicene, and azahelicene syntheses, *Angew. Chem., Int. Ed.*, 2006, **45**, 2242–2245.
45 D. P. Curran and A. I. Keller, Radical additions of aryl iodides to arenes are facilitated by oxidative rearomatization with dioxygen, *J. Am. Chem. Soc.*, 2006, **128**, 13706–13707.
46 R. R. Castillo, C. Burgos, J. J. Vaquero and J. Alvarez-Builla, Radical intramolecular arylation of pyridinium salts: A straightforward entry to 7-hydroxypyrido[2,1-*a*] isoquinolinylium salts, *Eur. J. Org. Chem.*, 2011, 619–628.
47 W. R. Bowman, A. J. Fletcher and G. B. S. Potts, Synthesis of heterocycles by radical cyclisation, *J. Chem. Soc., Perkin Trans. 1*, 2002, 2747–2762.
48 S. Saito, K. Matsuo and S. Yamaguchi, Polycyclic π-electron system with boron at its center, *J. Am. Chem. Soc.*, 2012, **134**, 9130–9133.
49 S. M. Allin, W. R. S. Barton, W. R. Bowman and T. McInally, Radical cyclisation onto pyrazoles: Synthesis of withasomnine, *Tetrahedron Lett.*, 2002, **43**, 4191–4193.
50 F. Filace, P. A. Sańchez-Murcia, D. Sucunza, A. Peŕez-Redondo, J. Álvarez-Buílla, F. Gago and C. Burgos, Silyl assistance in the intramolecular addition of pyridyl radicals onto pyridines and quinolines, *Eur. J. Org. Chem.*, 2016, 1891–1896.
51 For details see the ESI.†
52 J. Lalut, G. Santoni, D. Karila, C. Lecoutey, A. Davis, F. Nachon, I. Silman, J. Sussman, M. Weik, T. Maurice, P. Dallemagne and C. Rochais, Novel multitarget-directed ligands targeting acetylcholinesterase and σ1 receptors as lead compounds for treatment of Alzheimer's disease: Synthesis, evaluation, and structural characterization of their complexes with acetylcholinesterase, *Eur. J. Med. Chem.*, 2019, **162**, 234–248.
53 A. Ookawa, S. Yokoyama and K. Soai, Chemoselective reduction of diaryl bisulfides to thiols with sodium borohydride in mixed solvent containing methanol, *Synth. Commun.*, 1986, **16**, 819–825.
54 T. J. Burkey, M. Majewski and D. Griller, Heats of formation of radicals and molecules by a photoacoustic technique, *J. Am. Chem. Soc.*, 1986, **108**, 2218–2221.
55 M. J. Frisch, G. W. Trucks, H. B. Schlegel, G. E. Scuseria, M. A. Robb, J. R. Cheeseman, G. Scalmani, V. Barone, B. Mennucci, G. A. Petersson, H. Nakatsuji, M. Caricato, X. Li, H. P. Hratchian, A. F. Izmaylov, J. Bloino, G. Zheng, J. L. Sonnenberg, M. Hada, M. Ehara, K. Toyota, R. Fukuda, J. Hasegawa, M. Ishida, T. Nakajima, Y. Honda, O. Kitao, H. Nakai, T. Vreven, J. A. Montgomery, Jr., J. E. Peralta, F. Ogliaro, M. Bearpark, J. J. Heyd, E. Brothers, K. N. Kudin, V. N. Staroverov, R. Kobayashi, J. Normand, K. Raghavachari, A. Rendell, J. C. Burant, S. S. Iyengar, J. Tomasi, M. Cossi, N. Rega, J. M. Millam, M. Klene, J. E. Knox, J. B. Cross, V. Bakken, C. Adamo, J. Jaramillo, R. Gomperts, R. E. Stratmann, O. Yazyev, A. J. Austin, R. Cammi, C. Pomelli, J. W. Ochterski, R. L. Martin,

K. Morokuma, V. G. Zakrzewski, G. A. Voth, P. Salvador, J. J. Dannenberg, S. Dapprich, A. D. Daniels, O. Farkas, J. B. Foresman, J. V. Ortiz, J. Cioslowski and D. J. Fox, *Gaussian 09, Revision A.02*, Gaussian, Inc., Wallingford CT, 2009.

56 M. Cossi, G. Scalmani, N. Rega and V. Barone, New developments in the polarizable continuum model for quantum mechanical and classical calculations on molecules in solution, *J. Chem. Phys.*, 2002, **117**, 43–54, and references therein.

57 G. R. Fulmer, A. J. M. Miller, N. H. Sherden, H. E. Gottlieb, A. Nudelman, B. M. Stoltz, J. E. Bercaw and K. I. Goldberg, NMR chemical shifts of trace impurities: Common laboratory solvents, organics, and gases in deuterated solvents relevant to the organometallic chemist, *Organometallics*, 2010, **29**, 2176–2179.

58 L. Almanqur, I. Vitorica-yrezabal, G. Whitehead, D. J. Lewis and P. O'Brien, Synthesis of nanostructured powders and thin films of iron sulfide from molecular precursors, *RSC Adv.*, 2018, **8**, 29096–29103.